

# Coupled Oscillators with Chemotaxis

Satoshi SAWAI\* and Yoji AIZAWA

Department of Applied Physics, Waseda University, Tokyo 169-8555

(Received May 18, 1998 )

A simple coupled oscillator system with chemotaxis is introduced to study morphogenesis of cellular slime molds. The model successfully explains the migration of pseudoplasmodium which has been experimentally predicted to be lead by cells with higher intrinsic frequencies. Results obtained predict that its velocity attains its maximum value in the interface region between total locking and partial locking and also suggest possible roles played by partial synchrony during multicellular development.

KEYWORDS: coupled oscillators, cellular slime mold, morphogenesis

## §1. Introduction

Inspired by the collective behavior and rhythmicity of biological systems, synchronization of coupled limit-cycle oscillators with a frequency distribution has been studied using a system with all-to-all interaction in the following form,<sup>1,2,3)</sup>

$$\dot{W}_j = (i\omega_j + 1 - |W_j|^2)W_j + \frac{\epsilon}{N} \sum_{k=1}^N (W_k - W_j), \quad (1.1)$$

where  $\omega_j$  is an intrinsic frequency of the oscillator  $j$ ,  $W_j$  is a complex variable and  $(\dot{\phantom{x}}) = \frac{d}{dt}(\phantom{x})$ . The system has served well for theoretical studies on frequency entrainment and critical behaviors in a system far from equilibrium. Despite its original aim, however, very little has been discussed on the system's applicability and a connection to biological systems.

Development of the cellular slime mold *Dictyostelium discoideum* provides us with an ideal example that needs to be investigated in this respect, since its chemoattractant secretion exhibits limit-cycle oscillations in the vicinity of a Hopf bifurcation point<sup>4)</sup> with a difference in intrinsic frequencies and synchronization.<sup>5)</sup>

These eukaryotic cells feed on bacteria and grow by binary fission. Deprived of food, they initiate aggregation by emitting cAMP as a chemoattractant while simultaneously making a directed motion against its surrounding gradient. Each aggregation territory consists of  $10^3$  to  $10^5$  amoebae that together form a spherical mound whose nipple like apex zone consists of differentiated prestalk cells. The tipped mound elongates vertically to form a slug like pseudoplasmodium which migrates to a suitable environment where it forms a fruiting body.<sup>6,7)</sup>

To study a self-organizing process of cells in such systems, one must understand the nature of collective behavior in a population of motile oscillators. In the following, we first introduce a system that incorporates chemotaxis into eq. (1.1) and present the system's overall be-

havior. Then we discuss our results and their implications on development of a cellular slime mold.

## §2. Equations

The system is derived from a linear diffusion equation for two chemical species denoted by a complex variable  $Z(\mathbf{r}, t)$  and equations for chemotaxis of cell  $j$  at  $\mathbf{r} = \mathbf{r}_j$ . They are

$$\partial_t Z(\mathbf{r}, t) = D\nabla^2 Z(\mathbf{r}, t), \quad (2.1)$$

$$\dot{\mathbf{r}}_j(t) = \tilde{\alpha} \nabla \text{Re} Z(\mathbf{r}, t), \quad (2.2)$$

where  $D$  is a diffusion constant,  $\tilde{\alpha}$  is a chemotactic sensitivity coefficient.

Cell  $j$  ( $= 1, 2, \dots, N$ ) is represented by a region  $[0 \leq |\mathbf{r} - \mathbf{r}_j| \leq r_0]$  on which a boundary condition representing the metabolism  $\mathcal{F}$  of intracellular chemical species in a complex variable  $W_j(t)$  is imposed. The boundary conditions are expressed as

$$\lim_{r \rightarrow \infty} Z(\mathbf{r}, t) = 0, \quad (2.3)$$

$$Z(\mathbf{r}_j + \mathbf{r}_0, t) = W_j(t) + C, \quad (2.4)$$

$$\dot{W}_j(t) = \mathcal{F}(W_j) + \psi(\{W_k\}). \quad (2.5)$$

Here  $\psi(\{W_k\})$  is an abbreviation for the interaction term  $\psi(\{W_1, W_2, \dots, W_N\})$ , and  $C$  is a constant background level of  $Z(\mathbf{r}, t)$ . Solving eq. (2.1) under  $N$  boundaries (2.4) would yield a field  $Z(\mathbf{r}, t)$  in an integral equation

$$Z(\mathbf{r}, t) = \sum_{k=1}^N \int_0^t \Phi(|\mathbf{r}(t) - \mathbf{r}_k(\tau)|, t - \tau) (W_k(\tau) + C) d\tau, \quad (2.6)$$

where the diffusion kernel  $\Phi$  is either a Gaussian or Bessel-type function according to the dimension of  $\mathbf{r}$ .

In order to simplify the system, let us assume  $\Phi(|\mathbf{r}(t) - \mathbf{r}_k(\tau)|, t - \tau) \rightarrow \delta(t - \tau)$  in the limit of  $|\mathbf{r} - \mathbf{r}_k| \rightarrow 0$ . Assuming we had  $\mathcal{F}$  that yields the Hopf bifurcation normal form under a mean-field coupling  $\psi(\{W_k\}) \propto (Z(\mathbf{r}_j, t) - Z(\mathbf{r}_j + \mathbf{r}_0, t))$ ; eqs.(2.2) and (2.5) could be rewritten as

\* Present address: Research Institute of Electrical Communication, Tohoku University, Sendai 980-8577.

$$\dot{W}_j(t) = i\omega_j W_j(t) + (\lambda - |W_j(t)|^2)W_j(t) + \frac{\epsilon}{N-1} \sum_{k \neq j}^N \int_0^t \Phi(|\mathbf{r}_j(t) - \mathbf{r}_k(\tau)|, t - \tau) W_k(\tau) d\tau, \quad (2.7)$$

$$\dot{\mathbf{r}}_j = \frac{\alpha}{N-1} \sum_{k \neq j}^N \int_0^t \nabla \Phi(|\mathbf{r}_j(t) - \mathbf{r}_k(\tau)|, t - \tau) \text{Re}(W_k(\tau) + C) d\tau, \quad (2.8)$$

where  $\omega_j$  and  $\lambda$  independently determine the intrinsic frequency and the amplitude of the oscillation. In a weakly coupled regime, we could neglect the amplitude effect, therefore allowing eqs.(2.7) and (2.8) to be further reduced to a coupled phase model in the following form,

$$\dot{\phi}_j(t) = \omega_j + \frac{\epsilon}{N-1} \sum_{k \neq j}^N \int_0^t \Phi(|\mathbf{r}_j(t) - \mathbf{r}_k(\tau)|, t - \tau) \sin(\phi_k(\tau) - \phi_j(t)) d\tau, \quad (2.9)$$

$$\dot{\mathbf{r}}_j = \frac{\gamma(\phi_j)}{N-1} \sum_{k \neq j}^N \int_0^t \nabla \Phi(|\mathbf{r}_j(t) - \mathbf{r}_k(\tau)|, t - \tau) (\cos \phi_k(\tau) + c) d\tau + \mathbf{v}_d, \quad (2.10)$$

---

where  $c$  is the real part of  $C$ . In the transformation from eq. (2.7) to eq. (2.9), we have fixed  $\lambda = 1$ . In addition, the deceleration term and a periodic change of chemotaxis sensitivity were added to our previous model.<sup>9)</sup> Here, the sensitivity function  $\gamma$  and the short range interaction  $\mathbf{v}_d$  are defined by

$$\gamma(\phi) = \alpha(1 - \kappa \cos \phi), \quad (2.11)$$

$$\mathbf{v}_d = - \sum_{n \neq j}^N \frac{\beta}{(|\mathbf{r}_j(t) - \mathbf{r}_n(t)| - 2r_0)^2} \cdot \frac{\mathbf{r}_j(t) - \mathbf{r}_n(t)}{|\mathbf{r}_j(t) - \mathbf{r}_n(t)|}, \quad (2.12)$$

where  $\beta$  and  $\kappa$  are both positive constants.

By imposing a boundary condition on each cell that is in the form of an ordinary differential equation, the spatially extended system in eqs. (2.1) and (2.2) is now reduced to a set of integro-differential equations that tracks the time development of those cell boundaries. Notice that eq. (2.9) provides us with a general scheme that incorporates spatial dependency in the well-studied phase model.<sup>10,11)</sup> This is a novel approach to reaction-diffusion systems applicable to those that exhibit nonlinearity localized on boundaries.

### §3. Method

For the sake of numerical analysis, the kernel is simplified down to a point where it is not distinguishable from an one dimensional kernel except by the factor of  $\sqrt{\frac{r_0}{r}}$  and a shift in the origin of the exponent. Furthermore, it is multiplied by a step function which roughly incorporates the effect of degradation of the chemoattractant by the enzyme in the extracellular substratum. Therefore  $\Delta t$  could be considered as an average life span of the chemoattractant. The precise form used in the calculations is as follows:

$$\Phi(r, t - \tau) = \frac{\Theta(\tau - t + \Delta t)(r - r_0)}{\sqrt{4\pi D(t - \tau)^3}} \sqrt{\frac{r_0}{r}} e^{-\frac{r^2}{4D(t - \tau)}}, \quad (3.1)$$

where  $\Theta(t)$  denotes a Heaviside step function.

Numerical studies on eqs. (2.9) and (2.10) were performed using the fourth-order Runge-Kutta method in addition to the semiopen formula<sup>8)</sup> for the integral terms. Parameters  $D$ ,  $r_0$  and  $\kappa$  were fixed at unity throughout latter calculations. Other parameters are  $c = 2.0$ ,  $\omega_j = 1.0 + (j - 1)\Delta\omega$ ,  $\beta = 0.01$ ,  $\Delta t = 2.0$  unless stated otherwise.

We have employed constant initial values for the interval of  $[-\Delta t, 0]$ , and all results were obtained from a fixed step size of  $h=0.01$ . Some calculations where  $N = 2$  were checked for accuracy using  $h=0.001$  and  $h=0.0001$ .

### §4. Migration in $N = 2$

We will first describe the simplest case where  $N = 2$  to characterize attractors in the system. In order to carry out a steady-state approximation, chemotaxis will be confined to one dimension, and the adaptation will also not be considered ( $\kappa = 0$ ).

Suppose oscillators were entrained with a constant phase difference  $\psi = \phi_1 - \phi_2$ . When  $x_2 - x_1 = 2r_0 = \text{const.}$ , the equation describing the position of a centroid  $x_c = (x_1 + x_2)/2$  could be approximated by

$$\dot{x}_c \simeq \psi \alpha \int_0^t \nabla \Phi(2r_0, \tau') \sin \phi_1(t - \tau') d\tau', \quad (4.1)$$

where we have neglected the second- and higher-order terms of  $\psi$  and had a change in variable from  $\tau$  to  $\tau' = t - \tau$ . The mean cluster velocity  $v_c = \langle \dot{x}_c \rangle$  therefore would be proportional to  $\psi$ .

We see that  $v_c$  is also proportional to  $\Delta\omega$  from the locking condition  $\dot{\psi} = 0$ . Applying the same approximation as in eq. (4.1),

$$\dot{\psi} \simeq -\Delta\omega - 2\psi \epsilon \int_0^t \Phi(2r_0, \tau') \cos \omega^* \tau' d\tau', \quad (4.2)$$

where  $\omega^*$  is the entrained frequency. When the phase is locked,

$$\psi \simeq -\frac{\Delta\omega}{2\epsilon \int_0^t \Phi(2r_0, \tau') \cos \omega^* \tau' d\tau'} \quad (4.3)$$

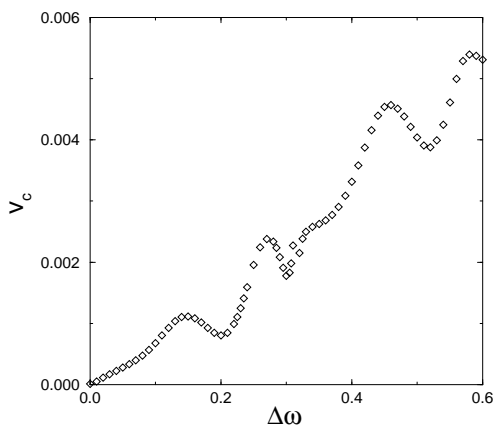


Fig. 1.  $\Delta\omega$  and the cluster velocity  $v_c$  ( $\omega_1 = 1.0, \omega_2 = \omega_1 + \Delta\omega, \epsilon = 1.0$  and  $\alpha = 1.0$ ).  $v_c$  was obtained using the method of least squares.

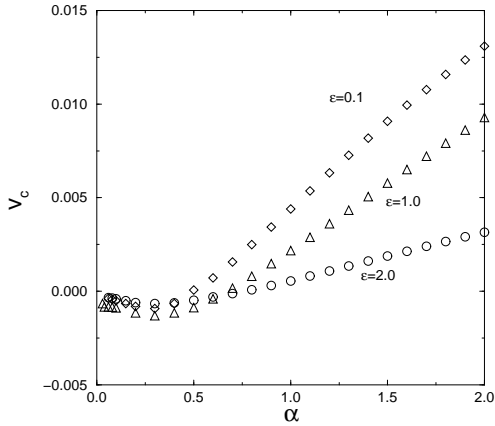


Fig. 2.  $\alpha$  and the cluster velocity for different  $\epsilon$  ( $\omega_1 = 1.0, \omega_2 = 1.1$  and  $\alpha = 1.0$ ). The initial condition was chosen so that  $x_1(0) < x_2(0)$ .

must be satisfied. From eqs.(4.1) and (4.3), one obtains  $|v_c| \propto \alpha\Delta\omega/\epsilon$ .

The parameter dependencies given here were confirmed by numerical simulations for  $N = 2$  with  $\kappa = 1.0$ . For a sufficiently large  $\alpha$ , the oscillator with larger  $\omega_j$  is advanced in phase and leads migration as one can see in Figs. 1 and 2. Not only  $\alpha$  but  $\Delta\omega$  also increases the cluster velocity  $v_c$ . Note that there is no net migration of a cluster when  $\Delta\omega = 0$ . Figure 2 also indicates that there is velocity proportional to  $\alpha$  (but not to  $1/\epsilon$ ) even when frequency is not entrained ( $\epsilon = 0.1$ ) due to the deceleration term which was not present in Aizawa-Kohyama (A-K) model discussed previously.<sup>9)</sup>

## §5. Numerical Results for $N = 20$

In order to characterize coherence in the phase dynamics, an order parameter  $R = \frac{1}{N} \sum_{j=1}^N e^{i\phi_j}$  is plotted against  $\epsilon$  in Fig. 3. Since we are dealing with a very small number of  $N$ ,  $|R|$  does not approach zero as  $\epsilon \rightarrow 0$ . Note

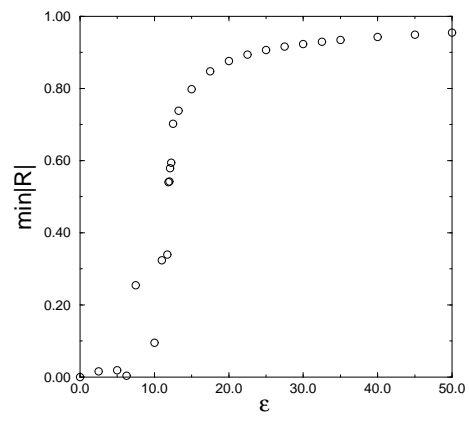


Fig. 3.  $\epsilon$  and the order parameter  $R$  ( $\alpha = 1.0$  and  $\Delta\omega = 0.01$ ). The minimum is plotted to withdraw fluctuations due to small  $N$ .

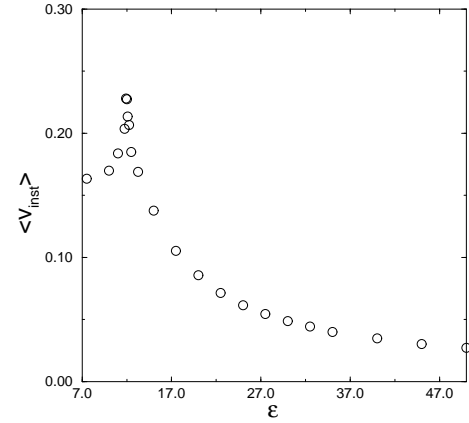


Fig. 4.  $\epsilon$  and cluster velocity ( $\alpha = 1.0$  and  $\Delta\omega = 0.01$ ).

that in Fig. 3, the minimum of  $|R|$  was plotted instead of, for example,  $\langle |R| \rangle$  ( $\langle \rangle$  denotes time averaging).

A cluster shows a directed migration when oscillators are entrained into a common frequency. The instantaneous velocity of a centroid defined by  $\mathbf{r}_c = \frac{1}{N} \sum_{j=1}^N \mathbf{r}_j$  is plotted against  $\epsilon$  in Fig. 4. The apparent discontinuity at the onset of total entrainment suggests that the cluster velocity, too, may be taken as an order parameter.

The relation between the polarity of a cluster and the migration direction could be understood by introducing  $Z(\theta)$  which is defined by

$$Z(\theta) = \sum_{k=1}^N k m_k(\theta), \quad (5.1)$$

where  $m_k$ s are natural numbers  $\{1, 2, 3, \dots, N\}$  representing the distance of oscillator  $j$  from a given point outside the cluster  $(x, y) = (r \cos \theta, r \sin \theta)$ ; 1 is assigned to the closest and 20 to the furthest oscillator. From the above definition,  $Z(\theta)$  takes the maximum value in the direction  $\theta$  (measured from the centroid) where oscillators with a smaller  $\omega_j$  are positioned.

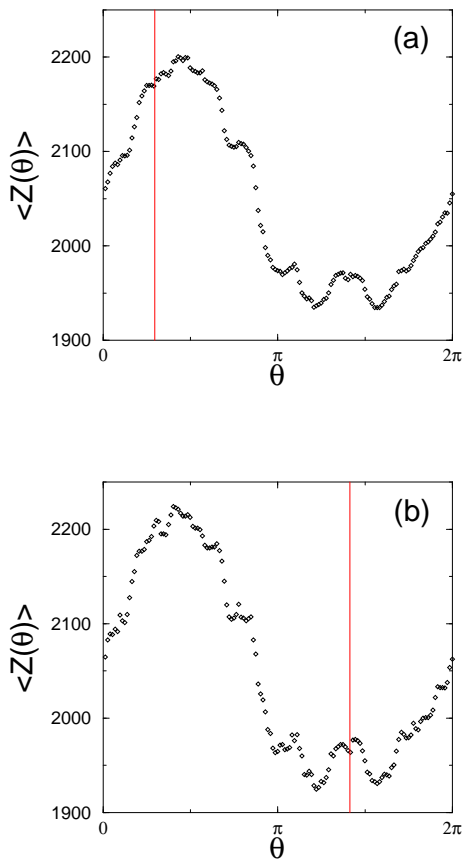


Fig. 5. Cluster polarity and migration direction ( $\epsilon = 30.0$ ,  $\alpha = 1.0$ ,  $\Delta\omega = 0.01$ ). Vertical lines indicate the direction of cluster migration. Other parameters are  $\Delta t = 2.0$  (a) and  $\Delta t = 6.0$  (b).

Figure 5 displays  $Z(\theta)$  and the direction of cluster migration. When  $\epsilon$  and  $\Delta t$  are small but large enough to synchronize oscillators, a cluster heads toward the direction where more oscillators with smaller  $\omega_j$  are located. The orientation reverses as both  $\epsilon$  and  $\Delta t$  are increased so as to make the coupling long range.

## §6. Discussion

A simple coupled oscillator model of cell aggregates was derived from a linear diffusion equation with time-dependent boundaries. The approximation in  $N = 2$  and numerical analysis carried out for  $N = 20$  revealed that synchrony in such a population of oscillators with chemotaxis results in migration as a whole. In addition to the migration direction that agrees with an experimental prediction, there are some implications from our present work concerning the possible order parameter.

We showed in Fig. 5 that in the case of  $N = 20$ , oscillators with larger  $\omega_j$  also lead the cluster translocation if  $\Delta t$  is sufficiently large. In the light of the prediction from suspension experiments<sup>5)</sup> that cells with higher frequency constitute the anterior of a slug, it may be concluded that cell to cell interaction is not local but rather long range. The opposite migratory direction predicted by a small  $\Delta t$  suggests that a reverse flow such as the

one exhibited by subpopulation of cells at the onset of culmination<sup>12)</sup> could be realized without any secondary chemoattractant. It would be interesting to see whether cells make use of such effect caused by different coupling ranges. This could be controlled either by the extracellular enzyme concentration or by the surface receptor occupancy.

The relation between the coupling strength  $\epsilon$  and the instantaneous cluster velocity has partly confirmed the result obtained by A-K model<sup>9)</sup> with its peak centered around the critical region. Below  $\epsilon = 7.5$ ,  $v_c$  continues to fluctuate with its direction not fixed which prevents us from obtaining its mean.

We have observed that in a partially synchronized state, locked oscillators emerge specifically in the anterior section of a cluster (data not shown) which implies that desynchronization plays a possible role in cell-type differentiation. In general,  $f^{-\mu}$  fluctuations are to be observed in such interface region. A detailed analysis on such fluctuation and its effect will be provided elsewhere.

Due to the coupling and chemotaxis in the form of integral equation, we have confined our present report on results obtained in the case of  $N = 20$  with fixed  $r_0$  and  $D$ . The diffusion characteristic makes it difficult to vary the ratio  $r_0^2/D$  since decreasing it requires smaller step size  $h$  and increasing it requires larger  $\Delta t$ . Future work will also address the construction of a simpler scheme that makes the analysis more feasible.

## Acknowledgements

We thank Prof. Y. Sawada for valuable discussions and remarks.

- 
- [1] Y. Aizawa: Prog. Theor. Phys. **56** (3) (1976) 703.
  - [2] R. E. Mirollo and S. H. Strogatz: J. Stat. Phys. **60** (1990) 245.
  - [3] P. C. Matthews, R. E. Mirollo and S. H. Strogatz: Physica D. **52** (1991) 293.
  - [4] Y. Tang and H. G. Othmer: Phil. Trans. R. Soc. Lond. B. **349** (1995) 179.
  - [5] C. J. Weijer, S. A. McDonald and A. J. Durston: Differentiation. **28**(1984) 9.
  - [6] Y. Maeda and K. Inouye: *Dictyostelium A Model System for Cell and Developmental Biology* (Universal Academy Press, Tokyo, 1997).
  - [7] W. F. Loomis: *The Development of Dictyostelium discoideum*. (Academic Press, New York, 1982).
  - [8] M. Abramowitz and I. Stegun: *Handbook of Mathematical Functions, Applied Mathematics Series*, Vol.55. (Dover Publications, New York, 1968).
  - [9] Y. Aizawa: Proceedings of 1st International Conference on Computing Anticipatory Systems, in press.
  - [10] Y. Kuramoto: *Lecture Notes in Phys.* **39** (1975) 420.
  - [11] H. Daido: Phys.Rev.Lett. **73**(5) (1994) 760.
  - [12] K. Jermyn, D. Traynor and J. Williams: Development **122** (1996) 753.